Research on Engineering Structures & Materials
journal homepage: http://www.jresm.org
MIM Research Group

Research Article

Manufacturing of testing specimens from tough HDPE-100 pipe: turning parameters optimization

Sabrina Mammeri[1,2,a], Kamel Chaoui[*1,b], Khaider Bouacha[1,c]

[1]*Mechanics of Materials and Plant Maintenance Research Laboratory (LR3MI), Mechanical Eng. Dept., Faculty of Technology, Badji Mokhtar University, P.O. Box 12, 23005, Annaba, Algeria*
[2]*Mechanical Eng. Dept., Faculty of Sciences and Technology, Mohamed-Chérif Messaadia University, P.O. Box 1553, Souk-Ahras 41043, Algeria*

Article Info

Article history:

Received 14 July 2023
Accepted 01 Nov 2023

Keywords:

HDPE pipe;
Tool geometry;
Machining;
Taguchi method;
Filament curvature;
Optimization

Abstract

Numerous machining operations are required in order to manufacture standard and non-standard specimens for mechanical testing of polymers. The present work focuses on the machinability of HDPE-100 pipe to prepare the utmost regular filaments with specified thickness and width. The study is set to establish mathematical correlations between surface quality (total roughness; Rt), cutting temperature ($T°$), filament uniformity (L) and corresponding cutting conditions. The latter include Vc (cutting speed), f (feed rate) and ap (depth of cut), combined with tool geometry (i.e., rake angle: γ and cutting-edge angle: κr). A mixed Taguchi L_{18} plan is adopted to organize and process the experimental runs. ANOVA and RSM (Response Surface Methodology) are employed to construct prediction models and optimize subsequent machining results. It is found that T (cutting temperature) and surface roughness criteria (Ra, Rt) are strongly affected by f and Vc. In addition, ANOVA results related to the height of filament bends (L) are likewise studied as a function of tool angles γ and κr. It is noted that cutting process is influenced by κr as it explains ~19% contributions of the total variation of parameter L, while γ, Vc and f show a little influence. It is deduced that optimum input parameters, represented by Vc, f, ap, γ and κr, are respectively 160 m/min, 0.5 mm/rev, 4 mm, (-6°) and 90° when turning tough HDPE material.

1. Introduction

Nowadays, countless polymer products are used for various daily life applications as substitutes for metallic materials because of technical advantages and economic considerations [1]. However, when adapting manufacturing techniques of metals to plastic materials, the reworked situations require rigorous and particular approaches for quality and strength control since polymer properties are usually lower than those of metallic components [2,3]. It is noted that polymer properties are essentially linked to their chemical structures, which determine a completely chaotic state (amorphous structure) or a partially ordered state (semi-crystalline structure). Such states allow specific properties in terms of flexibility and/or stiffness as well as resistance to common operating environments. Current standards requirements are actively contributing to ameliorate plastics processing methods and their integration especially into the piping industry [4]. This industry is dominated by high-density polyethylene (HDPE) pipes, which constitute an important underground substructure for water and natural gas distribution and transmission networks.

*Corresponding author: kamel.chaoui@univ-annaba.dz
[a] orcid.org/0009-0002-1961-8305; [b] orcid.org/0000-0001-6532-9462; [c] orcid.org/0000-0002-9349-5967
DOI: http://dx.doi.org/10.17515/resm2023.38ma0714rs

Although, plastics machining is not frequent compared to metals, it is becoming unavoidable as HDPE pipes are proposed for extreme applications such as contacts with hot, corrosive or radioactive fluids requiring new testing standards with substantial modifications. In most encountered machining cases, as described by Alauddin et al. [5], specific recommendations are discussed for orthogonal cutting, drilling, milling and grinding of thermoplastics. Usually, machining regime optimization for thermoplastics involves cutting regime parameters (i.e., speed, feed rate and depth of cut); however, additional controlling factors such as temperature, tool geometry and chip geometry may be taken into account in order to avoid structure alteration by thermal degradation [6] or large-scale deformations [7-10]. Salles and Gonçalves [8] studied the machining of UHMWPE (ultra-high molecular weight polyethylene) and surface quality parameters. They concluded that the observations made when turning such material are somewhat similar to the turning of aluminum and wood. Although many authors relate machinability of polymers to cutting speed, its influence on the surface finish in this case, is found to be insignificant. On the other hand, the cutting temperature does have great influence on final surface quality of this polymer [8].

Tamrin et al. [9] employed grey relational analysis for three different thermoplastics in order to determine an optimized set of machining parameters based on precision laser cutting. This process improves product quality and minimizes both service costs and operating errors. The ANOVA results show that such radiation power process has prevailing influence on the zone affected by heat generation for all studied thermoplastics. Silva et al. [10] investigated the precision turning of polyamide reinforced with 30% glass fiber as a function of feed rates and tool materials. They found that radial forces are the greatest, tailed respectively by cutting and feed ones. The polycrystalline diamond tool showed the lowest forces in relation to the best surface finish, followed by ISO uncoated carbide tool having a chip breaker. Irrespectively of the cutting regime parameters and tool material, continuous coiled microchips are produced in all checked cases. Chabbi et al. [11] examined machining parameters (*Vc*; *ap*; *f*) effects on force components, machine-tool power, roughness criteria and production as a function of time while turning POM-C (polyoxymethylene) polymer with a cemented carbide tool. Also, the analysis of output parameters includes a full factorial design (L27) followed by RSM and ANN techniques combined with desirability function optimization. From ANOVA analysis, it is concluded that *f* is the utmost significant factor influencing *Ra* with more than 66% contribution. However, tangential cutting force is mostly affected by *ap* and *f* parameters while the cutting power is evenly marked by the three main input cutting parameters. For minimal finish surface roughness issued from a turning process, the study gives 628 m/min, 0.08 mm/rev, and 1 mm as the optimized cutting parameters respectively for *Vc*, *f* and *ap*. For the turning process of PTFE (Polytetrafluoroethylene) polymer, Azzi et al. [12] analyzed the effects of input cutting regime parameters (i.e., *ap*; *f*; *Vc*) on roughness criteria (*Ra*, *Rz*) and material removal rate (MRR) using an L27 Taguchi design. Through ANOVA, it is concluded that *Ra*, *Rz* and MRR are effectively influenced by *f* (feed rate). The final optimization minimizing *Ra*, *Rz* and MRR, realized in the same way as in the previous study [11], gave a cutting regime with 270 m/min, 0.126 mm/rev and 2mm respectively for *Vc*, *f* and *ap.*

Kaddeche et al. [13] investigated surface finish, cutting forces and specifically cutting temperature changes while turning grade 80 and grade 100 polyethylene pipes materials. It is noticed that *f* (feed rate) is a dominant factor on roughness criteria and HDPE-80 roughness is much lower than that of HDPE-100. In addition, as anticipated from other studies, higher *Vc* values ameliorate surface quality nevertheless they increase cutting temperature leading to surface deterioration and material fusion. The other parameters are well discussed as a function of both pipe grades. Hamlaoui et al. [14] studied the

machining of HDPE-100 pipe for preparation of ISO specimens. They used RSM and desirability in order to assess the appropriate machining regime. They concluded that RSM and ANOVA approaches are suitable to describe the process of turning of HDPE-100 when considering both surface roughness and temperature measurements data as a function cutting regime conditions. Again, *f* remains as the most influencing parameter in order to minimize surface roughness for all the criteria, while *T* (temperature) is determined by *Vc* and *ap*. When considering temperature, the most secure case is given for 32°C which is a well-accepted upper bound by plastic pipe standards.

Fig. 1 shows a set of machined specimen geometries from HDPE pipe and which are considered for mechanical properties characterization. Fig. 1a exhibits typical gas pipe sections with yellow markings in the form of straight lines. It is possible to identify standard and non-standard specimens (Figs. 1b–1h) as machined from the pipe and respectively used for many testing conditions:

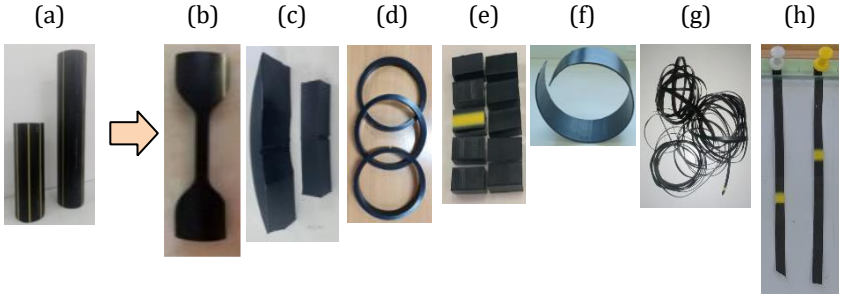

Fig. 1. Diverse testing specimen geometries machined from HDPE pipe

(b) tensile strength and creep; (c) impact fracture (Charpy); (d) residual stresses, (e) liquid sorption and (f) internal stresses relaxation. The last two cases are curled (g) and straight (h) filaments, continuously machined in a given direction, and are used to study mechanical and structural heterogeneities across pipe wall imparted by manufacturing processes [4,15-17]. Non-standard geometries are usually studied for specific applications and once technically approved by major pipe users; preliminary standards are prepared and put into standardized investigations to promote them as new standards. These specimen configurations serve different purposes and they include well-known ISO standards [4,16].

The objective of this study is to design appropriate machining conditions to obtain a uniform and continuous filament from an HDPE pipe. Later on, the filament will serve as specimens for mechanical testing and for investigating structure heterogeneity across the pipe wall. Aside from usual output machining parameters for plastics (i.e., roughness and temperature), minimizing filament curvature is considered as a criterion for filament geometrical uniformity. The study is based on RSM to construct correlations between input parameters (*Vc*, *f*, *ap*, *κr* and *γ*) and output ones which are cutting temperature (*T*), two roughness criteria (*Ra*, *Rt*) and filament curvature (*L*). Temperature and roughness values are predicted via the development of a second-order model through desirability. The analysis of variance method served to check the order of factor contributions to the cutting temperature.

2. Basic Approaches

The main goal of RSM is to optimize a process response when it is influenced by a number of variables. It has been successfully employed for many engineering production processes

[18-19]. According to literature [20-25], the RSM procedure is generally summarized in six different steps and is successfully applied in many experimental investigations available in literature [20-25].

Common relationships between input and output parameters are constructed via linear (1st order) and quadratic (2nd order) models as shown elsewhere [18-25]:

- First order model:

$$Y_k = a_0 + \sum_{i=1}^{n} a_i \cdot X_i + \varepsilon \quad (1)$$

where n is the number of variables and ε is item error.

- Second order model:

$$Y_k = a_0 + \sum_{i=1}^{n} a_i \cdot X_i + \sum_{i=1}^{n} a_{ii} \cdot X_i^2 + \sum\sum_{i<j}^{n} a_{ij} \cdot X_i \cdot X_j + \varepsilon \quad (2)$$

where Y_k is the desired output response, a_0 is constant, a_i, a_{ii} and a_{ij} are respectively, the coefficients of linear, quadratic and cross product terms. X_i are the coded variables.

Desirability (D) is a successful criterion for response optimization used to analyze polymer machining data or related others materials [14,18-25]. As a geometric mean of transformed responses, a nil D (i.e., D=0) reveals that selected response arrangement is just unacceptable. However, the proposed arrangement becomes an ideal case as D approaches unity (D≈1). D is defined as [20-25]:

$$D = \left(\prod_{i=1}^{n} d_i^{w_i} \right)^{\frac{1}{\sum_{j-1}^{n} w_i}} \quad (3)$$

where d_i and w_i are respectively the desirability and the weighting for the i^{th} targeted response. The number of responses for a given measuring position is termed n. Upper and lower limits should be given to each goal for a synchronized optimization.

The present study considers two surface roughness criteria (Ra and Rt), a cutting temperature (T) and a height of the filament bend (L) as output variables. The filament bend response is introduced after observing side filament curvature that is detrimental for mechanical properties measurements and should be lowered to a minimum. When searching for a minimum, the desirability limits are expressed as follows [18-23]:

$$\begin{cases} d_i = 1; & (if\ response\ < low\ value) \\ 1 \geq d_i \geq 0; & (if\ reponse\ varies\ from\ low\ to\ high) \\ d_i = 0, & (if\ response\ > high\ value) \end{cases} \quad (4)$$

In this optimization case, the combined advantages consist to have a good surface quality, the lowest cutting temperature and the less curved filament. Minimizing temperature is another essential requirement to avoid HDPE excessive heating and possible thermal degradation.

3. Experimental Procedure

The gas pipe material (HDPE-100), employed in this investigation, is pigmented with carbon black. Its external diameter (OD) is 200 mm and its thickness (t) is 11.4 mm (i.e.; SDR=17.6). Each work piece is 300 mm pipe portion (Figs. 1 and 2). This pipe is intended for the transportation and distribution of natural gas in urban areas. It is purchased from

the CHIALI Co. (Wilaya of Sidi Bel-Abbès, Algeria). It is designed according to European and Algerian standards (namely, EN 1555-2 and NA 7591-2) for medium pressure networks (4 bars) and can withstand tests from 6 to 10 bars gauge.

A succession of orthogonal turning operations is programmed on a tube work-piece (Fig. 2). A wooden mandrel is manufactured in order to reinforce holding the HDPE work-piece (Fig. 2a). Two mild-steel end caps are designed to secure both sides of the wooden tube-mandrel assembly to ensure eliminating any unwanted radial movement during operation (Fig. 2b). The dimensions of the basic system geometry and its machined parts are regular and verifiable throughout the experimental progression. Machining experiments are carried out in dry conditions using a parallel lathe (Type: SN-40; Spindle power: 6.6 kW). A commercially K20 carbide cutting tool is employed in this investigation as HDPE is a soft material and does not require special turning tool. Tool angles are selected within published polymer machining recommended intervals (γ: -6° and 15°; α: 6°; λ: 6° and κr: 30°, 60° and 90°) [7-14].

Roughness criteria (*Ra* and *Rt*) are measured via a roughness meter (Type: Surftest 301 Mitutoyo) as depicted in Fig. 2c. A calibrated special set-up is made in the lab to follow temperature changes using a developed application on a smart phone cell (Fig. 2d). In principle, for a given machined filament, the measurements are repeated 3 times and then averaged whenever needed. Usually, polymer chips or machining filaments are considerably distorted and sloped because of stresses and deformations imposed by cutting tool forward movements and work-piece rotation. From preliminary tests, Fig. 3 shows three (3) bent filament portions and two (2) relatively straight ones; both lots are obtained in different conditions (see also respectively, Fig. 1g and Fig. 1h).

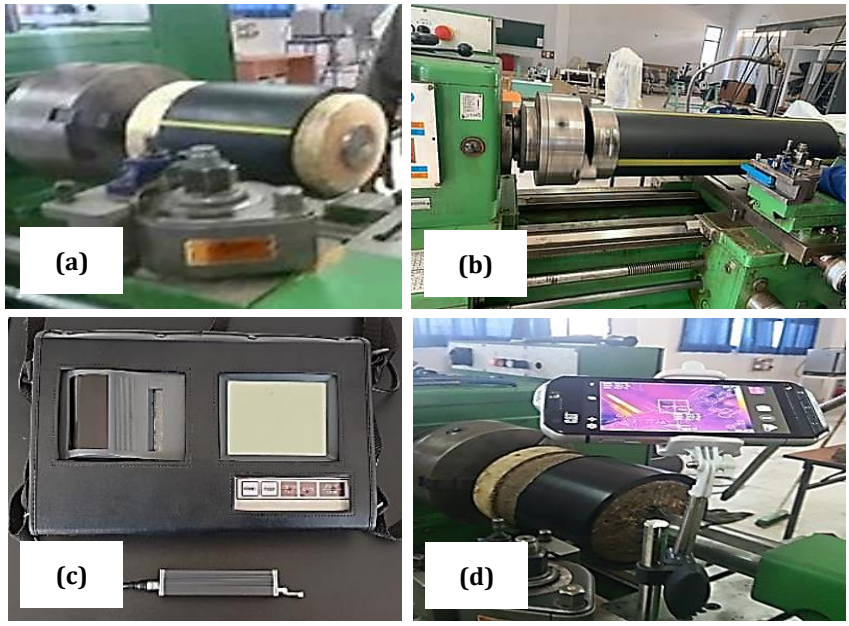

Fig. 2. Machining experimental setup

In order to allow performing acceptable tensile tests on such filaments, it is advised to minimize curliness upon machining. Therefore, a geometric criterion (L) is also combined with output parameters in order to lessen filament lateral curvature. For instance, a similar approach is employed in the case of milling of polymers to control burr height that may

limit the field of technical applications. Usually, this extra chip (or burr) of material is the result of plastic deformation due to the cutting process and is highly influenced by feed rate and other parameters for micro-milling of thermoplastic PMMA (polymethylmethacrylate) [26-28]. Parameter L is measured, in the same specific conditions, using the normal deviation from a 70 mm length of tangent to the filament (Fig. 3a).

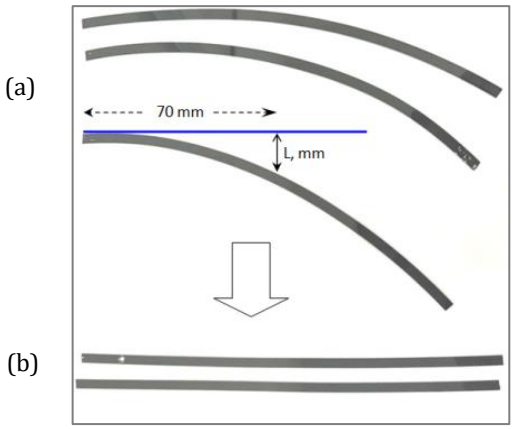

Fig. 3. Description of L parameter from low contrast photos of machined HDPE filaments; (a) large and (b) very low curvature

In order to initiate the study, an experimental design is chosen. It consists of 18 runs as explained in section 4.1 and it is based on three levels and five factors (i.e.; machining parameters) as reported in Table 1.

In this specific work, the polymer chips are intended to serve as mechanical test specimens for a subsequent study of properties heterogeneity imparted by the extrusion process of the HDPE pipe. Thus, the main imposed conditions on the process of obtaining the filament comprise continuity and regularity of the chip, a cutting temperature below 40°C and the least possible deformations. Finally, the manufacturing process of the desired final specimen configuration should take advantage from optimal machining parameters.

Table 1. Levels of the cutting regime input parameters

Level	Vc	f	ap	γ	κr
	(m/min)	(mm/rev)	(mm)	(°)	(°)
1	100	0.37	2	−6	30
2	140	0.53	3	-	60
3	560	0.67	4	15	90

It is established that opposite effects govern the influence of speed (Vc) on both temperature and surface quality. In this scenario, it is advantageous to keep a relatively high cutting speed, but this does not help lowering cutting temperature as stated in polymer machining guidelines [29,30]. Carr and Feger [7] showed that the roughness of a thermoplastic polyimide as a function of the speed Vc or the rake angle γ passes through a minimum established by laboratory tests.

Consequently, the process variables and the 3 levels are selected inside the working limits proposed and published by tool manufacturers research studies dedicated to

thermoplastics [7,9,10-12,29,30]. In this study, this critical phase is corroborated with some preliminary laboratory trials and available experimental literature dedicated to HDPE machining [6,8,13,14]. It is understood that selected process variables have pronounced effects on the quality of output characteristics, forming the three levels adopted herein.

4. Results and Discussion

4.1 Experimental Planning (Taguchi L_{18})

The performance characteristics (cutting temperature, total and arithmetic mean surface roughness criteria, and height of the filament bend) are measured after turning operations using Taguchi L_{18} mixed level. The results are exhibited in Table 2 and output data suggest that the highest cutting temperature (39.6°C) is recorded at the highest levels of *Vc* and *f*. Viscous friction during polymer material removal is strongly active in heat generation. In fact, the cutting temperature corresponding to these machining conditions (Run No.3, Table 2) is very close to the upper limit temperature allowed by standards for HDPE materials (i.e.; 40°C). Inversely, lower cutting speeds of 100 m/min and lower values f and *ap* are associated with much lower temperatures (28.5°C) but not always with required roughness criteria [13,14,29,30]. On the other side, the highest filament height bend (7.5mm) seems to be favored by higher *Vc*, *f* and *ap*. This state illustrates severe and intense machining conditions for semicrystalline polymers and is in direct relationship with cutting temperature changes [31]. At this stage, it is concluded that the upper limit parameters of level 3, especially *Vc* and *f* (Table 1) cannot be optimized values.

4.2 Analysis of Variance (ANOVA)

Based on experimental data, ANOVA results are used to identify input factors which significantly affect performance parameters. Table 3 presents this analysis for the cutting temperature (Table 3a), the surface roughness criteria (Tables 3b-3c) and the logarithmic height of the filament bend, *Ln(L)*, (Table 3d).

Table 2. Input and output data based on (L_{18})

Run N°	Cutting Parameters					Performance Characteristics			
	Vc (m/min)	*f* (mm/rev)	*ap* (mm)	*γ* (°)	*κr* (°)	*T* (°C)	*Ra* (µm)	*Rt* (µm)	*L* (mm)
1	100	0.37	2	-6	30	28.5	0.97	0.61	4.3
2	140	0.53	3	-6	30	32.9	1.18	0.74	3.8
3	560	0.67	4	-6	30	39.6	0.98	0.52	7.5
4	100	0.67	3	-6	60	32.3	1.44	0.78	1.5
5	140	0.37	4	-6	60	31.7	0.81	0.39	1.3
6	560	0.53	2	-6	60	35.8	0.86	0.42	1.4
7	100	0.53	2	-6	90	31.1	1.05	0.60	1.1
8	140	0.67	3	-6	90	33.4	1.29	0.69	1.3
9	560	0.37	4	-6	90	32.8	0.41	0.14	0.5
10	100	0.53	4	15	30	30.7	1.39	0.75	2.9
11	140	0.67	2	15	30	32.6	1.55	0.97	1.2
12	560	0.37	3	15	30	33.5	0.69	0.32	2.4
13	100	0.67	4	15	60	32.4	1.42	0.89	5.2
14	140	0.37	2	15	60	29.6	0.96	0.48	1.8
15	560	0.53	3	15	60	34.8	0.92	0.51	1.6
16	100	0.37	3	15	90	28.5	0.64	0.41	2.7
17	140	0.53	4	15	90	30.8	0.95	0.53	4.3
18	560	0.67	2	15	90	36.2	1.41	0.63	1.9

It is found that subsequent models are satisfactory. Principal significant factors are rake angle (γ), cutting-edge angle (κr), and regime parameters (Vc, f and ap).

Table 3a. ANOVA of cutting temperature

Label	DF	Seq SS	CP%	Adj SS	Adj MS	F-tests	P-value
Model	8	128.777	98.10	128.777	16.0971	58.07	0.000
Linear	5	122.478	93.30	121.873	24.3746	87.94	0.000
γ	1	4.500	3.43	4.500	4.5000	16.24	0.003
κr	1	2.083	1.59	3.120	3.1197	11.26	0.008
Vc	1	74.427	56.70	70.380	70.3804	253.92	0.000
f	1	39.998	30.47	41.995	41.9947	151.51	0.000
ap	1	1.470	1.12	1.653	1.6530	5.96	0.037
Square	1	2.228	1.70	2.228	2.2277	8.04	0.020
$Vc*Vc$	1	2.228	1.70	2.228	2.2277	8.04	0.020
2-way interaction	2	4.071	3.10	4.071	2.0356	7.34	0.013
$\kappa r *Vc$	1	1.861	1.42	1.726	1.7260	6.23	0.034
$Vc*f$	1	2.211	1.68	2.211	2.2106	7.98	0.020
Error	9	2.495	1.90	2.495	0.2772		
Total	17	131.271	100.00				

From Tables 3a–3c, T, Ra and Rt are intensely affected by f and Vc. The most significant factor on the parameters Ra and Rt remains f explaining respectively 51.92% and 63.67% contributions of the overall discrepancy. Next major contribution on Ra and Rt is dictated by Vc with respectively, 29.45% and 15.89% the contributions.

Table 3b. ANOVA of Ra

Label	DF	Seq SS	CP%	Adj SS	Adj MS	F-tests	P-value
Model	6	0.71800	98.19	0.71800	0.119666	99.70	0.000
Linear	5	0.70398	96.28	0.67429	0.134859	112.36	0.000
γ	1	0.02000	2.74	0.02000	0.020000	16.66	0.002
κr	1	0.06901	9.44	0.04674	0.046744	38.94	0.000
Vc	1	0.21531	29.45	0.21531	0.215313	179.39	0.000
f	1	0.37965	51.92	0.37965	0.379646	316.30	0.000
ap	1	0.02001	2.74	0.01483	0.014831	12.36	0.005
2-way interaction	1	0.01402	1.92	0.01402	0.014021	11.68	0.006
$\kappa r*Vc$	1	0.01402	1.92	0.01402	0.014021	11.68	0.006
Error	11	0.01320	1.81	0.01320	0.001200		
Total	17	0.73120	100.00				

Table 3c. ANOVA of Rt

Label	DF	Seq SS	CP%	Adj SS	Adj MS	F-tests	P-value
Model	8	1.68662	98.87	1.68662	0.210827	98.02	0.000
Linear	5	1.55005	90.86	1.32176	0.264352	122.90	0.000
γ	1	0.04909	2.88	0.04909	0.049089	22.82	0.001
κr	1	0.08501	4.98	0.03699	0.036987	17.20	0.002
Vc	1	0.27101	15.89	0.28786	0.287864	133.83	0.000
f	1	1.08614	63.67	0.88167	0.881667	409.89	0.000
ap	1	0.05880	3.45	0.01507	0.015065	7.00	0.027
2-way interaction	3	0.13657	8.01	0.13657	0.045525	21.16	0.000
$\kappa r*Vc$	1	0.07199	4.22	0.09001	0.090008	41.85	0.000
$\kappa r*f$	1	0.04514	2.65	0.03722	0.037218	17.30	0.002
$\kappa r*ap$	1	0.01944	1.14	0.01944	0.019441	9.04	0.015
Error	9	0.01936	1.13	0.01936	0.002151		
Total	17	1.70598	100.00				

For the cutting temperature, cutting speed (Vc) is in first position with a contribution of 56.70% followed by f explaining 30.47% of overall discrepancy. Table 3d presents the ANOVA results corresponding to the height of the filament bends (L) as a function of process parameters (γ, κr, Vc, f and ap). It is shown that the main effects of these process parameters are all significant with respect to the height of the filament bends. While, the most significant process parameter is the cutting-edge angle (κr), which explains 18.99% contributions of the total variation, followed by the depth of cut (ap) (6.56 %).

Moreover, it can be realized that γ, Vc and f show a relatively small influence on the height of the filament bends. However, for rake angle (γ), cutting-edge angle (κr) and depth of cut (ap) interactions, influence degrees are very important in comparison to the remaining terms, especially, for rake angle (γ) and cutting-edge angle (κr), which explains 40.78%.

In Fig. 4, main effects deduced from this study are sketched out. It should be noted that overlooked variables are supposed to be kept constant around an averaged value bounded by two assumed levels. They indicate that T is significantly affected by two regime parameters namely Vc and f as per Fig. 4a. In addition, the graphs reveal that, whenever Vc and f increase, corresponding cutting temperature increases as expected.

Nevertheless, for polymeric materials, cutting speed remains an important input parameter. Indeed, any increase in Vc, inevitably will lead to a rise in T because friction dominates in the so-called "second shear zone". Conversely, at lower cutting speed, lower heat is generated and results in lessened temperatures values [14]. Similarly, when f increases, the filament section and the deformed material volume increase and hence the temperature increases, particularly, in the first shear zone by deformation [23].

Obviously, it is noted that Ra and Rt criteria are highly affected by f as shown in Figs. 4b and 4c. Usually technical literature accepts that parameter f or its squared form (f^2) have a cumulative effect on the geometric surface roughness criteria.

Table 3d. ANOVA of Ln(*L*)

Label	DF	Seq SS	CP%	Adj SS	Adj MS	F-tests	P-value
Model	11	7.61434	99.63	7.61434	0.69221	146.38	0.000
Linear	5	2.72088	35.60	2.85707	0.57141	120.83	0.000
γ	1	0.33220	4.35	0.65938	0.65938	139.43	0.000
κr	1	1.45100	18.99	1.08021	1.08021	228.42	0.000
Vc	1	0.19806	2.59	0.23008	0.23008	48.65	0.000
f	1	0.23788	3.11	0.08199	0.08199	17.34	0.006
ap	1	0.50174	6.56	0.85242	0.85242	180.25	0.000
Square	2	0.19429	2.54	0.75633	0.37816	79.97	0.000
*Vc*Vc*	1	0.17789	2.33	0.52553	0.52553	111.13	0.000
*f*f*	1	0.01640	0.21	0.65735	0.65735	139.00	0.000
2-way interaction	4	4.69917	61.49	4.69917	1.17479	248.42	0.000
*γ*κr*	1	3.11632	40.78	3.50141	3.50141	740.42	0.000
*γ*ap*	1	0.61899	8.10	1.45922	1.45922	308.57	0.000
*κr*ap*	1	0.46017	6.02%	0.77480	0.77480	163.84	0.000
*Vc*ap*	1	0.50369	6.59	0.50369	0.50369	106.51	0.000
Error	6	0.02837	0.37	0.02837	0.00473		
Total	17	7.64271	100.00				

(a)

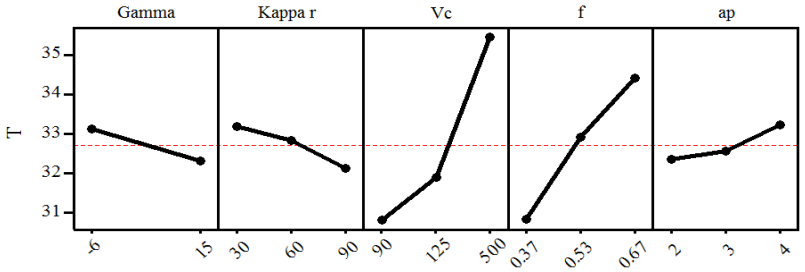

(b)

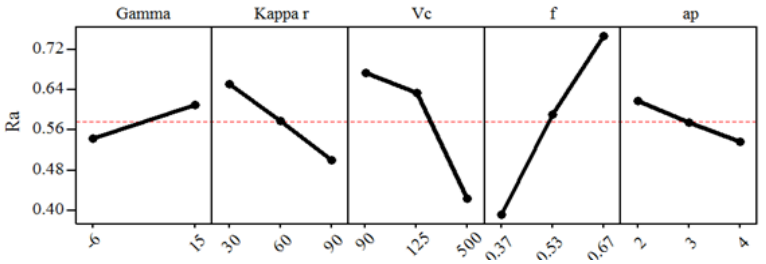

(c)

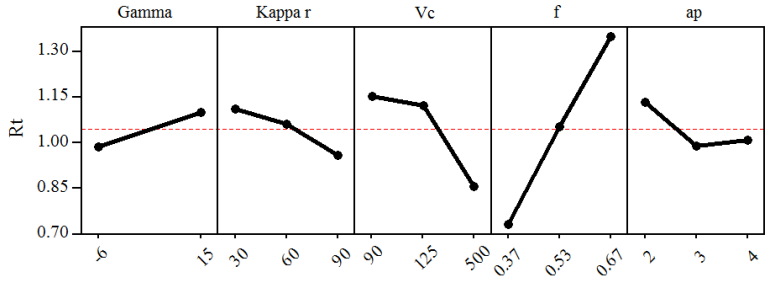

(d)

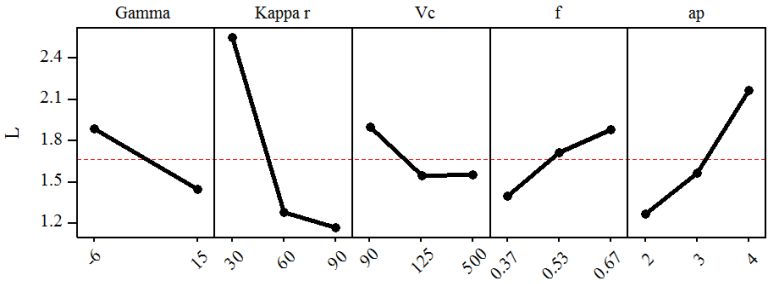

Fig. 4 Principal effect-plots for outputs : (a) *T*, (b) *Ra*, (c) *Rt* and (d) *L*

Parameter *Vc* is associated with important trend variations. For instance, surface roughness is progressively perfected by increasing *Vc*. In cutting processes, it is also well known that higher cutting speed leads to a better surface finish while the deformation velocity influences, to some extent, the residual properties of the workpiece material. It is also accepted that the higher the speed, the less substantial the plastic comportment is. The flow of plastically deformed lateral material of the workpiece along cutting-edge direction can enhance peaks heights and valleys depths of surface irregularities [13,14,23,32]. As shown in Fig. 4d, height of the filament bends (*L*) decreases considerably with the decrease of the cutting-edge angle (*κr*). Additionally, it should be emphasized that uncut chip thickness is explained by means of the combined effects of parameters *f*, *ap* and *κr*. In other words, as the angle *κr* is reduced, the chip width is enlarged. The latter is a direct consequence of cutting-edge active span increase. This results in an intensification of the heat amount taken away from the cutting zone by chip formation and hence, the chip deformation and height of the filament bends increase. However, as the cutting-edge angle (*κr*) increases, the amount of heat evacuated by the chip is lessened and the spiral-shape chip tends to form. This results in a decrease in the height of the filament bends. No significant changes are observed on the performance characteristics because of variations in the rake angle (*γ*), since it mainly influenced the tool nose resistance.

4.3 RSM Models

The relationship between process parameters (*Vc, f, ap, γ* and *κ)* and performance characteristics (*T*, *Ra*, *Rt* and *L*) are correlated using RMS. Each prediction model is developed at 95% confidence level with Minitab 19 experimental design software and it is based on regression analysis using least square method.

The initial regression equations of the performance characteristics are based on input parameters and corresponding interactions. It should be noted that the RSM can be also used to obtain an exponential model through the natural logarithmic transformation of a

process parameter and its performance characteristics. The following equations for performance characteristics are obtained (Eqs. 5-8):

$$T = 21.28 - 0.048\,\gamma + 0.003\,\kappa r + 0.04\,Vc + 8.41f - 0.384\,ap - 0.005 * 10^{-2}\,Vc^2 - 0.006 * 10^{-2}\,\kappa r * Vc + 0.014\,Vc * f\,; \quad [R^2 = 98.10\%] \tag{5}$$

$$Ra = 0.429 + 0.318 * 10^{-2}\,\gamma - 0.004\,\kappa r - 0.0009\,Vc + 1.145f - 0.356\,ap + 0.006 * 10^{-3}\,\kappa r * Vc; \quad [R^2 = 98.19\%] \tag{6}$$

$$Rt = 0.883 + 0.005\,\gamma - 0.009\,\kappa r - 0.149 * 10^{-2}\,Vc + 0.946\,f + 0.075\,ap + 0.014 * 10^{-2}\,\kappa r * Vc + 0.017\,\kappa r * f - 0.002\,\kappa r * ap; \quad [R^2 = 98.87\%] \tag{7}$$

$$L = e^{\left(\begin{matrix}4.977 - 0.2967\,\gamma + 0.02381\,\kappa r + 0.02256\,Vc - 29.13\,f + 0.3747 ap - 0.000039 Vc^2 + \\ 28.58\,f^2 + 0.001750\,\gamma * \kappa r + 0.07055\,\gamma * ap - 0.01396\,\kappa r * ap + 0.001313\,Vc * ap\end{matrix}\right)}; \quad [R^2 = 99.63\%] \tag{8}$$

These RSM models are applicable only within stated range levels according to Table 1. High percents of R^2-values (98.10% ÷ 99.63%) for equations (5) to (8) indicate consistent appraises for each described output parameter. Based on the Anderson-Darling normality test, it is shown that calculated probabilities of residual variations as a function of predicted responses follow closely a straight line as plotted in Fig. 5.

Concerning *Ra*, *Rt* and *T*, as shown in Figs. 5a-c, the corresponding *P*-values (0.513; 0.982; 0.415) are above the 5% significance level, implying a normal distribution. For the height of chip/filament bend case, data linearization required a normalization using the logarithmic transformation and A-D test *P*-value for *L* and *Ln(L)* increased respectively from 0.013 to 0.579 as shown in Fig. 5d [33]. The corresponding determination coefficients (R^2) indicate very satisfactory correlations.

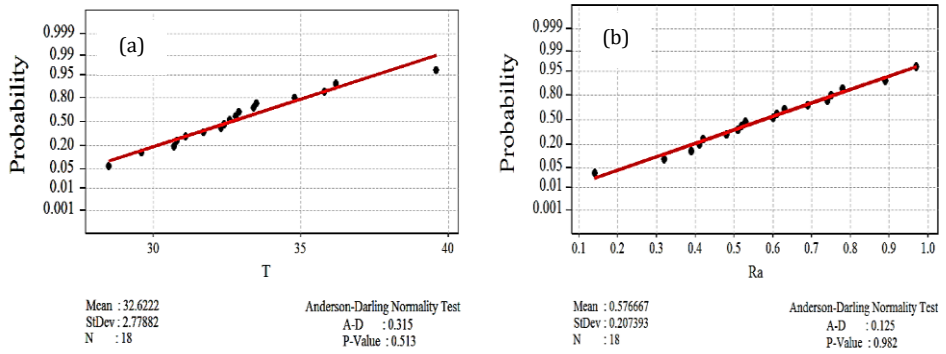

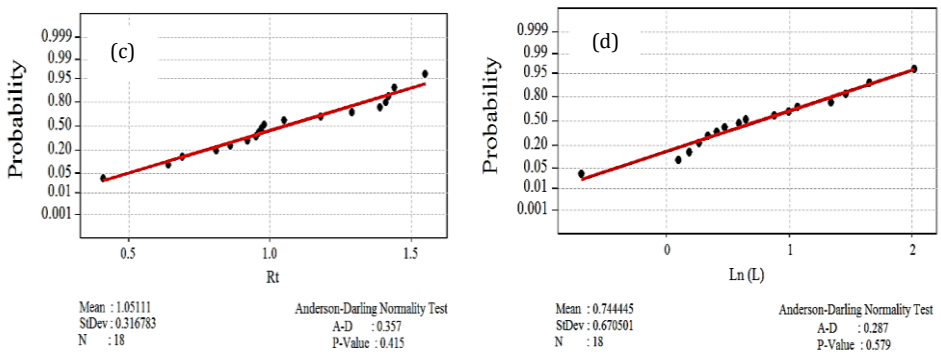

Fig. 5. Normal probability plots for: (a) *T*°, (b) *Ra*, (c) *Rt* and (d) *Ln(L)*

4.4 RSM 3-D Plots

Significant combined effects of the process factors are selected and illustrated in Figs. 6-9 in the form of 3-D responses surface plots respectively for *T*°, *Ra*, *Rt* and *Ln(L)*. Figs. 6a-b show the effects of *Vc*, *f* and cutting-edge angle (*κr*) on measured machining temperature. It is observed that the cutting speed effect is the highest compared to that of *f* and *κr*. The cutting temperature increase is explained by the frictional activities at the chip-tool cutting interface. The maximum value of temperature is reached within the 350 to 550 m/min cutting speed range.

Most significant interactions are found between *Vc* and *f*, where the lowest cutting temperature is accomplished with the lowest *Vc* and the lowest *f* combinations (Fig. 6b). At lower cutting speeds, it is also observed that no important changes affected the cutting

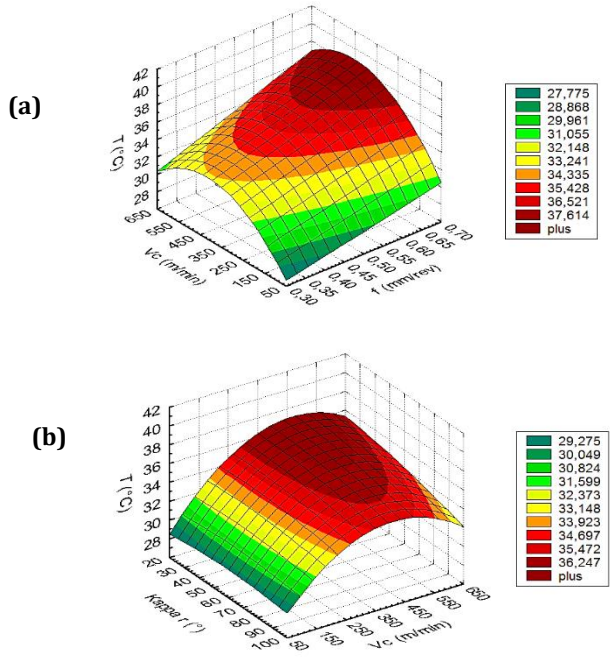

Fig. 6. Response surface for cutting T° as a function of: (a) *Vc* and *f*; (b) *κr* and *Vc*

temperature because of cutting-edge angle variations (Fig. 6b). When turning HDPE pipe material with a high-speed steel tool, Hamlaoui et al. [14] found that the cutting temperature is principally affected by *Vc* and *ap* as compared to *f*. The introduction of cutting-edge angle gave a better insight on *T* variations.

Estimated response surface plots for *Ra* and *Rt* as a function of parameters (*Vc*, *f*, *ap* and the angle *κr*) are illustrated in Figs. 7-8. In Fig. 7, it can be seen that *Vc* has the greatest influence on *Ra* and its discrepancy is high when compared to that caused by cutting-edge angle. Also, Fig. 7 shows that *Ra* is improved by increasing cutting speed as expected. No substantial changes are observed for *Ra* due to cutting-edge angle variations at higher *Vc*. Conversely, for lower cutting speed values, *κr* effect becomes important. The best surface roughness quality in terms of *Ra* is achieved at the highest cutting-edge angle and the highest cutting speed combination. This is a new finding compared to results of previous studies [13,14].

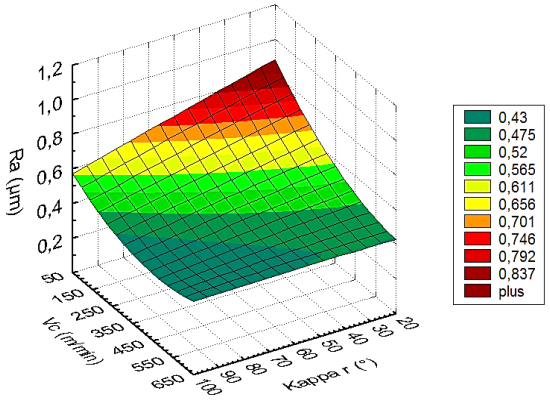

Fig. 7. Response surface for Ra as a function of *Vc* and *κr*

Fig. 8 presents the variations of roughness criterion *Rt* as function cutting regime parameters (*Vc, f, ap*) and cutting-edge angle. In Fig. 8a, it is observed that higher depth of cut and higher cutting-edge angle significantly improved *Rt* by almost two folds (from 1.3 down to ~0.63µm). This corroborates the previous results discussed in the *Ra* case.

The Figs. 8a-b show the maximum opposite effects on *Rt* caused by increasing *ap* and *f*. At the highest cutting-edge angle, the variation *Rt* is 75% at the lower limits of *ap* and *f* (i.e., 1.8 mm and 0.30 mm/rev) and only 55% at the upper limits (i.e., 4.2 mm and 0.70 mm/rev). The best *Rt* value (0.3 µm) is obtained for a feed rate of 0.3 mm and a maximum cutting-edge angle. As expected, higher feed rates contribute to extensive deformations of the machined polymer surface and on the evacuated chip. In addition, Fig. 8b suggests that *Rt* is around 1.4 µm and almost independently of *κr* for the highest feed rate.

A similar behavior is observed for the variation of *Rt* as function of cutting speed and cutting-edge angle (Fig. 8c). It is observed that highest roughness values (~1.4 µm) are obtained for lowest cutting-edge angles and the lowest cutting speed. It is understood that cutting time is long enough to cause extensive deformation at the machined surface under the tool action. On the other side, when *κr* is increased for low speeds *Rt* is slightly ameliorated (~0.92µm).

Globally, at the highest *κr*, *Rt* becomes almost constant as a function of *Vc*. It is concluded that the best combination is obtained when *κr* is the lowest and *Vc* is the highest (*Rt*~ 0.5µm) which is three folds lower than that of 50 m/min. The best surface quality, expressed in terms of *Rt*, is achievable combining the highest *κr* with either the lowest *f* or the lowest *ap*. Moreover, the most significant interactions are found between *f* and *κr*.

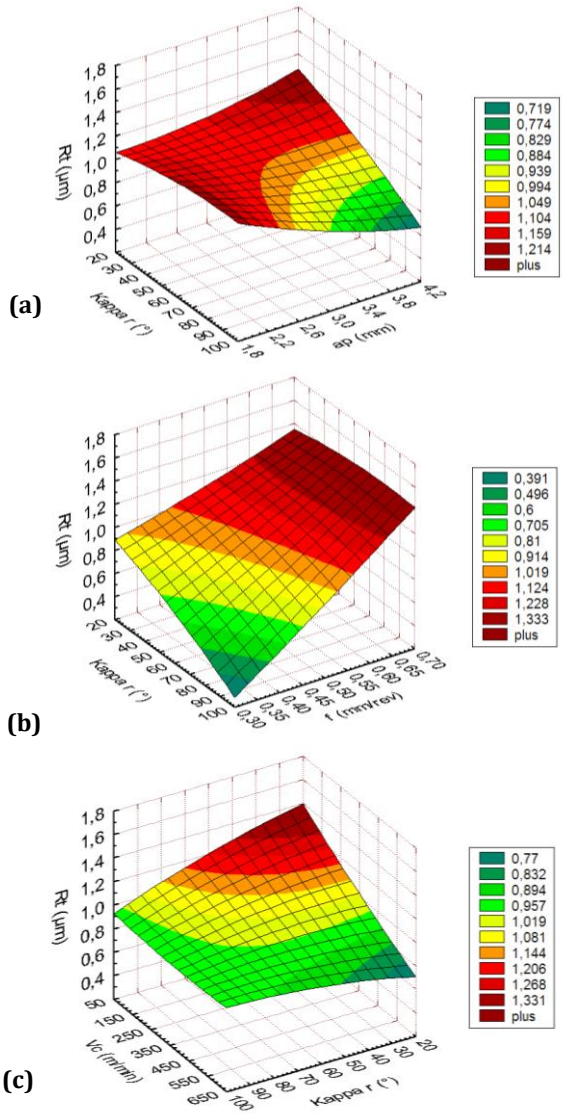

Fig. 8 Response surface for Rt as a function of: (a) *κr*, *ap;* (b) *κr*, *f*; (c) *Vc*, *κr*

Fig. 9 presents chip/filament curvature parameter, which has been defined earlier in Section 3, as a function of *ap*, *Vc* and *κr*. From Fig. 9a, it can be seen that cutting-edge angle has the highest decreasing effect on filament height bend. No really significant changes are observed on the filament height bend values as a function of *ap* variation especially at higher cutting-edge angles and higher cutting speeds (Fig. 9a-b). The possible explanation is in relation to the generated heat at the interface chip-cutting tool which softens cut

material as discussed earlier. A rise in *Vc* between 100 and 350 m/min, increased the interface tool-chip temperature regardless of *f* and *κr* values (Fig. 6).

As a result, there is a decrease of maximum shearing forces within the shear area and at the tool-chip interface. Furthermore, the shearing angle is increased and, at the same time, the chip thickness is lessened. It follows, the filament will tend to be ribbon-shaped as the contact area tool-chip becomes smaller. Beyond this limit (350 m/min), as cutting speed increases, the filament height bend increases and subsequently, it becomes more curved. The best uniform filament can be achieved with the highest cutting-edge angle and *Vc* in the interval 350–450 m/min. There is agreement between RSM 3-D plots and experimental results.

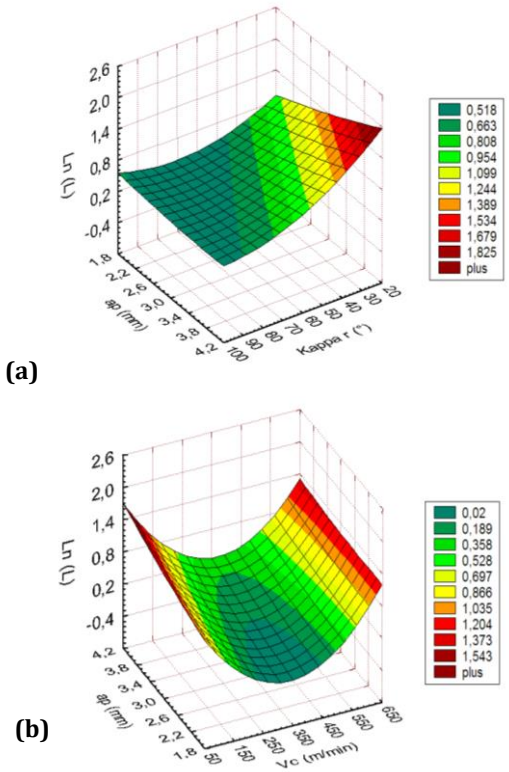

Fig. 9 Response surface for *Ln(L)* as a function of: (a) *ap*, *κr* and (b) *ap*, *Vc*

4.5 Optimization Using Composite Desirability

A principal goal for an experimental approach is to help investigate optimal values for the cutting parameters. In this case, regime parameters become the desired values for the sought output parameters during HDPE pipes turning process. In other words, the use of RSM helps identifying the arrangement of input (geometric and regime) parameters (i.e., *γ*, *κr*, *Vc*, *f* and *ap*) that conjointly optimize cutting temperature, surface roughness criteria and the lowermost filament bend height. As defined in [24], the composite desirability (D) is the resultant of weighted geometric individual desirabilities. In order to reduce machined filament dimensional deviations, cutting parameters are restricted within bottom and top permissible limits as applied in various studies [11,12,14,20,23,]. There

are several factors restraining the cutting process parameters for HDPE pipe material and some of them have been quoted in published literature [5,13,14,17].

The limitations taken into account, in the case of HDPE, cover 4 categories in relation to: *(i)* cutting regime, *(ii)* tool geometry, *(iii)* surface quality and *(iv)* upper limit temperature. They are given by the inequalities (9-16):

$$(i)\begin{cases} 100 \le Vc \le 560 & (9) \\ 0.48 \le f \le 0.52 & (10) \\ 3.9 \le ap \le 4.0 & (11) \end{cases}$$

$$(ii)\begin{cases} -6° \le \gamma \le +15 & (12) \\ +30° \le \kappa r \le +90° & (13) \end{cases}$$

$$(iii)\begin{cases} Ra \le 0.24\ \mu m & (14) \\ Rt \le 0.59\ \mu m & (15) \end{cases}$$

$$(iv)\ \begin{cases} T \le 34°C & (16) \end{cases}$$

The optimized solution without any constraints for *T*, *Ra*, *Rt* and *Ln(L)* is given Tables 4a and 4b. All responses are rated with the same weight and importance since there is no indication to opt for different schemes. Table 4a shows the results of RSM optimization without constraints for targeted values of cutting temperature *(T)*, surface roughness criteria *(Ra, Rt)* and logarithmic height of the filament bend *(Ln(L))*. Later on, the lowest value of *L* is extracted and examined. For the optimal desirability, the proposed technical solution is given in Table 4b. It clearly displays tool angles as stated in literature, i.e., a negative γ and a maximum κr. However, *Vc* remains high and such condition can affect drastically the obtained filaments since they are not massive and bulky like machined parts capable of evacuating most generated heat.

Table 4a. Parameters for optimized solution without constraints

Response	Goal	Lower	Target	Upper	Weight	Importance
Ln (L)	Minimum	-	-0.693	2.015	1	1
Ra	Target	0.140	0.240	0.970	1	1
Rt	Target	0.410	0.590	1.550	1	1
T	Target	28.5	34.0	39.6	1	1

Table 4b. Optimized solution with constraints for *T*, *Ra*, *Rt* and *Ln(L)*

γ	κr	*Vc*	*f*	*ap*	*Ln(L)*	*Ra*	*Rt*	*T*	Composite Desirability
-4.497	90	550.014	0.438	3.831	-0.693	0.240	0.590	34.0	1.000

It should be noted that the corresponding value for parameter L is 0.5 mm. Alternatively, the corresponding calculated responses optimization for output parameters are summarized in Fig. 10.

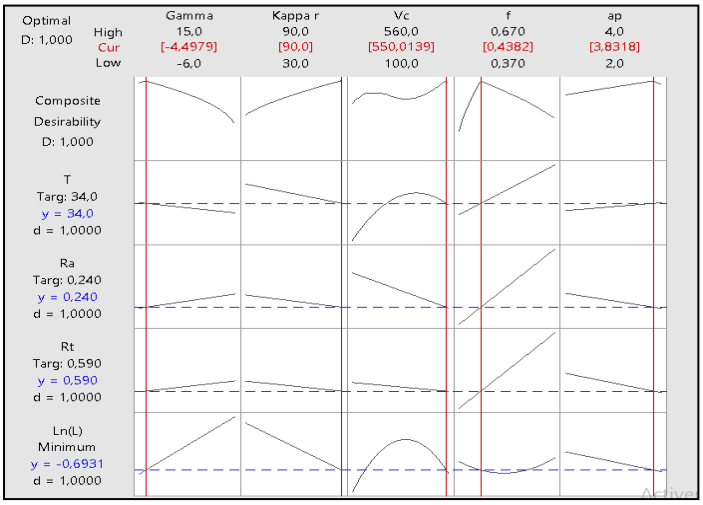

Fig. 10 Recapitulation of response optimization without constraints

Likewise, Tables 5a and 5b illustrate the results of RSM optimization with constraints and Fig. 11 gives the corresponding response optimization for the output parameters. From preliminary tests, temperature variations can be under control using optimized feed rate and cutting speed. The remaining difficulties concern especially L and to some extend Ra. For these reasons, importance and weight indices are maximized for both $Ln(L)$ and Ra as shown in Table 5a. $Ln(L)$ and Ra are set respectively at 6 and 5 times the weights (and importance) of T or Rt in order to reduced filament curvature and approach a more or less a rectilinear shape.

Table 5a. Parameters for optimized solution with constraints

Response	Goal	Lower	Target	Upper	Weight	Importance
Ln (L)	Minimum	-	-0.693	2.015	6	6
Ra	Target	0.140	0.460	0.970	5	5
Rt	Target	0.410	0.820	1.550	1	1
T	Target	28.5	33.0	39.6	1	1

Table 5b. Optimized solution with constraints for T, Ra, Rt and $Ln(L)$.

γ	κr	Vc	f	ap	$Ln(L)$	Ra	Rt	T	Composite Desirability
-6	90	160.225	0.515	4	-1.227	0.460	0.821	32.98	0.9995

In the machining guidelines of polymers, it is usually recommended that cutting edges should have generous relief angles (i.e., important cutting-edge angles) associated to negative back rake angle in order to keep at a minimum any eventual rubbing and/or abrasion action. These recommendations contribute to ameliorate surface roughness during machining. In the present case, both κr (≤90°) and γ (-6°) are in adequate intervals

for the machining of HDPE. Another important conclusion deals with the relatively reduced cutting speed (160 m/min) which is acceptable as an equilibrated level between *T* and *Ra* requirements. The corresponding obtained actual value of *L* is 0.293 mm which largely sufficient when testing in traction soft and bendable filaments.

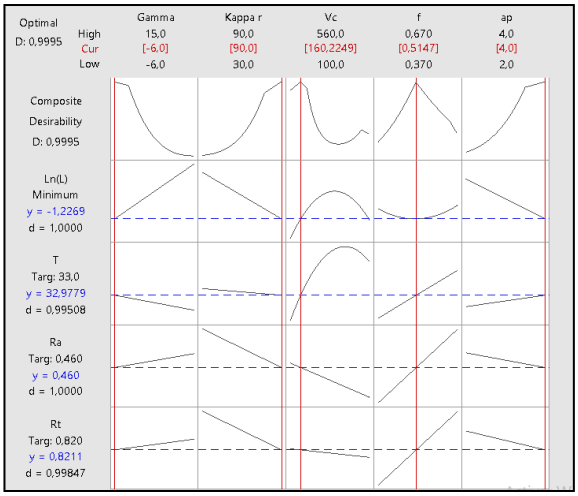

Fig. 11. Recapitulation of response optimization with constraints

The other important parameter is temperature which is well below the 40°C upper limit. The value of *ap* is intentionally kept high enough as it will serve as a built-in geometric dimension of the filament during testing. It should be noted that the corresponding value for parameter *L* is 0.293 mm.

4.6. Analysis of Predicted Results

The analysis of predicted results is a necessary step in order to decide on the optimization validity. Figs. 12 (a-d) summarize the variances between experimental and modeled responses for *T*, *Ra*, *Rt* and *Ln(L)* respectively. It is found that quadratic models can basically characterize the machining system under these experimental conditions.

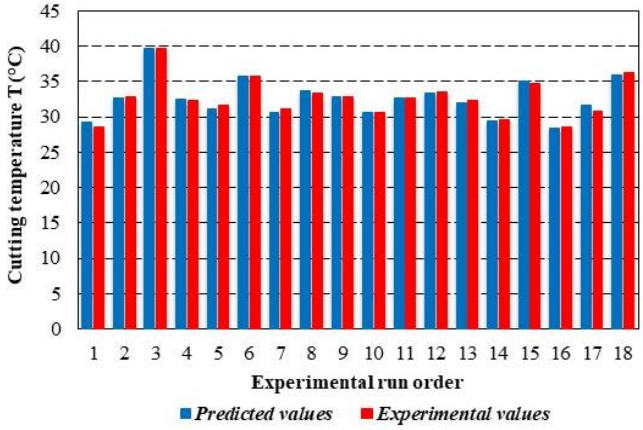

(a)

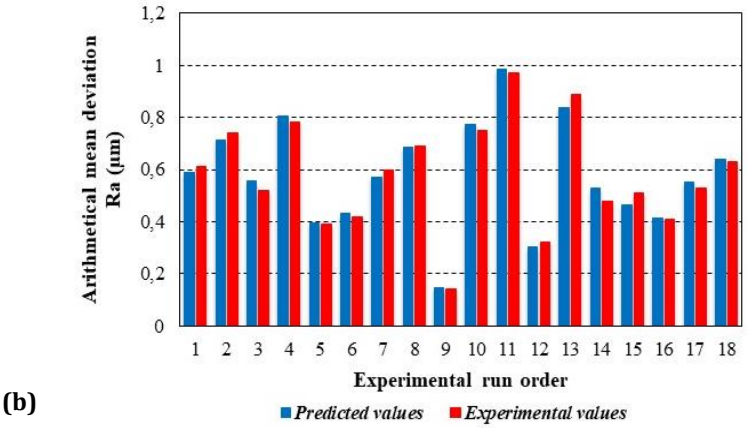

(b)

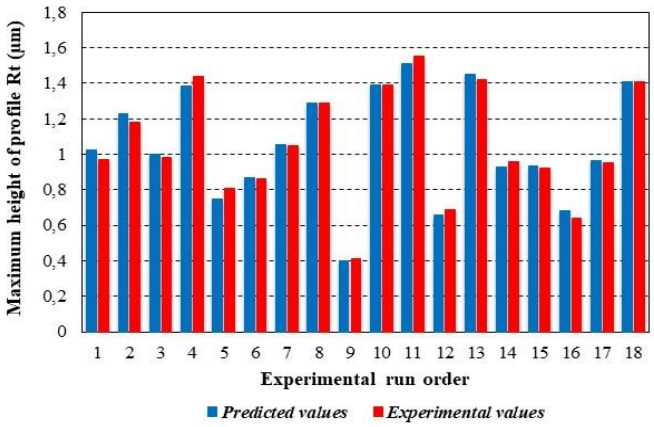

(c)

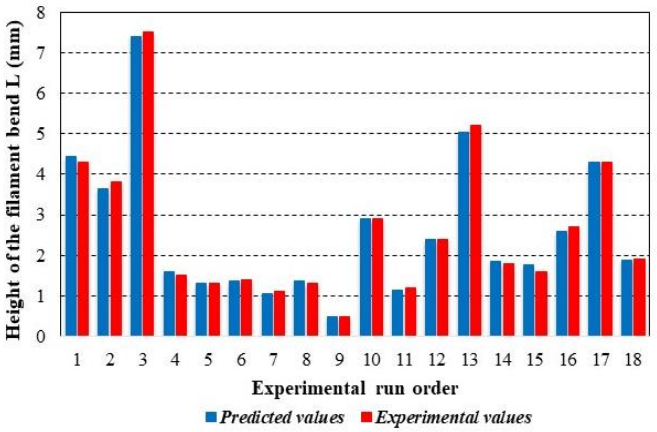

(d)

Fig. 12 Experimental and predicted data for: (a) *T*, (b) *Ra*, (c) *Rt* and (d) *L*

For semi-crystalline materials that exhibit both viscous and elastic characteristics when undergoing machining operations, both composite desirability and quadratic models can be employed for multi-objective optimizations. It is noted that HDPE is a thermoplastic with very low glass transition and melting temperatures. Literature indicates that viscous properties of HDPE play a considerable effect on the machined surface quality as viscous

deformation is critically relying on both strain rate and cutting temperature [6,31]. In other words, disproportionate viscous–plastic scaling or tearing, at a high *Vc*, can be drastically limited by evacuating the heat generated by friction. The effects of rake angle (γ), feed rate (*f*) and some molecular properties are also discussed for others polymers [25-28,31,32].

5. Conclusion

This work is intended to ameliorate previous studies dedicated to the optimization of machining conditions of HDPE pipes to manufacture mechanical testing specimens [13,14]. Both studies [13] and [14] were undertaken respectively in 2012 and 2017, using a conventional Tagushi approach, together with ANOVA and desirability analyses for HDPE-80 and HDPE-100. However; in this study, the number of input and output parameters is extended to cover respectively cutting tool geometry and ultimate shape of the machined filament (chip). The main conclusions are:

- Besides usual cutting parameters regime (*Vc*, *f* and *ap*), the effects of both rake (γ) and cutting-edge (κr) angles are considered as supplementary input parameters. Conversely, for output parameters, a new information representing the height of bends (*L*) is recorded to appraise the machined filament curvature along with cutting temperature and roughness criteria.
- It is found that *f* and *Vc* are strongly affecting temperature (*T*) and surface roughness criteria (*Ra*, *Rt*). When considering the total variation of *Ra* and *Rt*, the effects of *f* explained respectively 51.92% and 63.67% of the contributions. The limited effects of *Vc* revealed only 29.45% and 15.89% respectively for *Ra* and *Rt*.
- Alternatively, for cutting temperature, *Vc* effects come is in the first position followed by those of feed rate with respectively 56.70% and 30.47% contributions of the total variation. Graphically, it is deduced that as *Vc* and *f* increase, T increases as expected. For polymeric semicrystalline materials, it is accepted that *Vc* remains the most important input parameter and the temperature rise is caused particularly in the second shear zone where friction dominates. Similarly, when *f* increases, the filament section and the deformed material volume increase and hence the temperature increases, particularly in the first shear zone by deformation. The maximum value of the cutting temperature is reached within the 350 to 550 m/min cutting speed range.
- Concerning the newly introduced parameter, i.e.; height of the filament bends (*L*), it is shown that the main effects of process factors are all significant but at different degrees. The most significant one remains the cutting-edge angle (κr), which explains 18.99% contributions of the total variation, followed by the depth of cut (*ap*) with 6.56 %. Also, it is found the height of the filament bends (*L*) decreases considerably with the increase of the cutting-edge angle (κr). It is explained that as the cutting-edge angle (κr) increases, the amount of heat evacuated by the out-going chip is lessened and the spiral-shape filament is likely to form.
- The RSM models allowed to predict the performance characteristics for any combination of factor levels for the adopted ranges. The Anderson-Darling test for normality indicates that predicted responses for *T*, *Ra*, *Rt* and *Ln(L)* follow normal laws.
- The validation experiments demonstrate that the obtained mathematical models allowed to correctly predict cutting temperature, surface roughness criteria and filament height bend values within a 95% confidence interval. Very satisfactory determination coefficients (>98%) are noted.

- The best optimized solution is obtained with imposing high constraints on output parameters (*L* and *Ra*). It is revealed that *Vc*=160 m/min (as a main input) and a filament bend height *L*=0.293mm (as a main output) are reasonable and most practical conditions for a regular and uniform filament. In addition, the proposed solution is favored with a generous cutting-edge angle (*κr*) combined with a negative back rake angle (*γ*) which helps keeping at a minimum both rubbing and abrasion actions.
- Finally, the multi-objective optimization approach based on the composite desirability technique and quadratic RSM models is shown to be an adequate method to control performance characteristics when machining tough HDPE pipe materials.

Acknowledgements

This study is a part of the work program defined for the PRFU Research Project "*Mechanical behavior and remaining life of HDPE pipes subjected to operating and environmental conditions*"; Code A11N01UN230120190008; LR3MI, UBM Annaba, Algeria. This project is supported by DGRSDT-MESRS (Algerian Ministry of Higher Education and Scientific Research).

Nomenclature

AD:	Anderson-Darling normality test.
ap:	Depth of cut (mm)
D:	Desirability
DL:	Degrees of freedom
f:	Feed rate (mm/rev)
F:	Fisher test
L:	Filament height bend (or curvature) (mm).
P:	Error value compared at 5.
P-value:	Probability value
R^2:	Determination Coefficient
Ra:	Arithmetic mean roughness (μm)
Rt:	Total roughness (μm)
RSM:	Response Surface Methodology
SDR:	Pipe diameter to thickness ratio
T:	Temperature (°C)
Vc:	Cutting speed (mm/min)

Greek Letters:

α :	Clearance angle (°);
γ:	Rake angle (°)
κr:	Cutting-edge (or steering) angle (°)
λ:	Cutting edge inclination angle (°).

References

[1] Nguyen QK, Mwiseneza C, Mohamed K, Cousin P, Robert M, Benmokrane B. Long-term testing methods for HDPE pipe - advantages and disadvantages: A review. Eng. Fract. Mech., 2021; 246: 107629. https://doi.org/10.1016/j.engfracmech.2021.107629

[2] Jagtap UT, Mandave AH. Machining of Plastics: A Review. Int. J. Eng. Res. & Gen. Sci., 2015; 3(2): 577-581. www.ijergs.org

[3] Berneck J. Plastics instead of metals. Kunststoffe International, 2012; 9: 57-59. www.kunststoffe-international.com

[4] Handbook of *Polymer Testing: Short-Term Mechanical Tests. The Rubber and Plastics Specialists*, Editor: Brown R., Rapra Technology Limited, UK, 2002. http://www.rapra.net
[5] Alludin M, Choudhury IA, El Badarie MA, Hashmi MSJ. Plastics and their machining: A review, J. Mater. Proc. Technol, 1995; 54(1-4): 40-46. https://doi.org/10.1016/0924-0136(95)01917-0
[6] Kaiser MS, Fazlullah F, Ahmed SR. A comparative study of characterization of machined surfaces of some commercial polymeric materials under varying machining parameters. J. Mech. Eng., Automation & Control Syst, 2020; 1(2): 75-88. https://doi.org/10.21595/jmeacs.2020.21643
[7] Carr WJ, Feger C. Ultraprecision machining of polymers. 1993; 15, 4: 221-237. https://doi.org/10.1016/0141-6359(93)90105-J
[8] Salles JLC, Gonçalves MTT. Effects of machining parameters on surface quality of the ultra-high molecular weight polyethylene (UHMWPE). Materia, 2002; 8 (1): 1-10. http://www.materia.coppe.ufrj.br/sarra/artigos/artigo10119/10119.pdf
[9] Tamrin KF, Nukman Y, Choudhury IA, Shirley S. Multiple-objective optimization in precision laser cutting of different thermoplastics. Optics and Lasers in Engineering, 2015; (67): 57-65. https://doi.org/10.1016/j.optlaseng.2014.11.001
[10] Davim JP, Silva LR, Festas A, Abrão AM. Machinability study on precision turning of PA66 polyamide with and without glass fiber reinforcing. Materials and Design, 2009; 30(2): 228-234. https://doi.org/10.1016/j.matdes.2008.05.003
[11] Chabbi A, Yallese MA, Nouioua M, Meddour I, Mabrouki T, Girardin F. Modeling and optimization of turning process parameters during the cutting of polymer (POM C) based on RSM, ANN, and DF methods, Int. J. Adv. Manuf. Technol, 2017; 91: 2267–2290. https://doi.org/10.1007/s00170-016-9858-8
[12] Azzi A, Boulanouar L, Laouisi A. Modeling and optimization of machining parameters to minimize surface roughness and maximize productivity when turning polytetrafluoroethylene (PTFE). Int. J. Adv. Manuf. Technol. 2022; 123: 407–430. https://doi.org/10.1007/s00170-022-10160-z
[13] Kaddeche M, Chaoui K, Yallese MA. Cutting parameters effects on the machining of two high density polyethylene pipes resins, Mechanics & Industry, 2012; 13(5): 307-316. https://doi.org/10.1051/meca/2012029
[14] Hamlaoui N, Azzouz S, Chaoui K, Azari, Yallese MA. Machining of tough polyethylene pipe material: surface roughness and cutting temperature optimization. Int. J. Adv. Manuf. Technol. 2017; 92, 5(8): 2231-2245. https://doi.org/10.1007/s00170-017-0275-4
[15] Niglia J, Cisilino A, Seltzer R, Frontini P. Determination of impact fracture toughness of polyethylene using arc-shaped specimens. 2002; 69 (12):1391-1399 https://doi.org/10.1016/S0013-7944(02)00008-5
[16] Broughton WR, Maxwell AS. Ageing of polymeric materials, A National Measurement Good Practice Guide. 2007:103. https://eprintspublications.npl.uk/3866/1/mgpg103.pdf
[17] Kiass N, Khelif R, Bounamous B, Amirat A, Chaoui K. Experimental study of mechanical and morphologic al properties in HDPE-80 gas pipe. Mechanics & Industry, 2006; 7: 423-432. https://doi.org/10.1051/meca:2006056
[18] Bouacha K, Yallese MA, Mabrouki T, Rigal JF. Statistical analysis of surface roughness and cutting forces using response surface methodology in hard turning of AISI 52100 bearing steel with CBN tool. Int. J. Refract. Met. & Hard Mater. 2010; 28(3): 349–361. https://doi.org/10.1016/j.ijrmhm.2009.11.011
[19] Davoodi B, Eskandari B. Tool wear mechanisms and multi-response optimization of tool life and volume of material removed in turning of N-155 iron-nickel-base superalloy using RSM. Measurement. 2015; 68: 286-294. https://doi.org/10.1016/j.measurement.2015.03.006

[20] Gutema EM, Gopal M, Lemu HG. Temperature Optimization by Using Response Surface Methodology and Desirability Analysis of Aluminum 6061. Materials. 2022; 15(17): 5892. https://doi.org/10.3390/ma15175892
[21] Parida AK, Routara BC, Bhuyan RK. Surface roughness model and parametric optimization in machining of GFRP composite: Taguchi and Response surface methodology approach. Materials Today: Proceedings. 2015; 2(4-5): 3065–3074. https://doi.org/10.1016/j.matpr.2015.07.247
[22] Subramanian AVM, Nachimuthu MDG, Cinnasamy V. Assessment of cutting force and surface roughness in LM6/SiC_p using response surface methodology. J. Appl. Res. & Technol. 2017; 15(3): 283–296. https://doi.org/10.1016/j.jart.2017.01.013
[23] Chabbi A, Yallese MA, Meddour I, Nouioua M, Mabrouki T, Girardin F. Predictive modeling and multi-response optimization of technological parameters in turning of Polyoxymethylene polymer (POM C) using RSM and desirability function. Measurement, 2017; 95: 99-115. https://doi.org/10.1016/j.measurement.2016.09.043
[24] Derringer G, Suich R. Simultaneous optimization of several response variables. J. Qual. Technol. 1980; 12(4): 214-219. https://doi.org/10.1080/00224065.1980.11980968
[25] Khuri AI. Mukhopadhyay S. Response surface methodology. WIREs Computational Statistics, 2010; 2(2): 128-149. https://doi.org/10.1002/wics.73
[26] Yan Y, Mao Y, Li B, Zhou P. Machinability of thermoplastic polymers: PEEK, PI, and PMMA. Polymers (Basel), 2020; 13 (1): 69-83. https://doi.org/ 10.3390/polym13010069
[27] Reichenbach IG, Bohley M, Sousa Fabio FJP, Aurich Jan C. Micromachining of PMMA—manufacturing of burr-free structures with single-edge ultra-small micro end mills Int. J. Adv. Manuf. Technol., 2018; 96:3665–3677. https://doi.org/10.1007/s00170-018-1821-4
[28] Giasin K, Ayvar-Soberanis S. An Investigation of Burrs, Chip formation, Hole Size, Circularity and Delamination during Drilling Operation of GLARE using ANOVA, Composite Structures, 2016; 159:745-760. http://dx.doi.org/10.1016/j.compstruct.2016.10.015
[29] Mitsubishi Chemical Group. Guide To Machining Plastic Parts, Metric System. Machinist's Toolkit. (Consulted on 6 Sept. 2023) https://www.mcam.com/mam/41701/MCG-Machinist-Toolkit-A4-EU-metric.pdf
[30] Curbell Plastics, Inc. Plastic Turning Machining Guidelines. (Consulted on 6 Sept. 2023) https://www.curbellplastics.com/services-capabilities/fabrication-machined-parts/plastic-machining-guidelines/plastic-turning-machining-guidelines/
[31] Xiao KQ, Zhang LC. The role of viscous deformation in the machining of polymers. Int. J. Mech. Sci, 2002; 44 (11): 2317-2336. https://doi.org/10.1016/S0020-7403(02)00178-9
[32] Alateyah AI, El-Taybany Y, El-Sanabary S, El-Garaihy WH, Kouta H. Experimental Investigation and Optimization of Turning Polymers Using RSM, GA, Hybrid FFD–GA, and MOGA Methods. Polymers, 2022; 14 (17): 3585-3610. https://doi.org/10.3390/ polym14173585
[33] Yap BW, Sim CH. Comparisons of various types of normality tests. J. Statistical Computation and Simulation, 2011; 81(12): 2141-2155 http://dx.doi.org/10.1080/00949655.2010.520163